

## Analytical Time Optimal Control Solution for a Two-Link Planar Acrobat with Initial Angular Momentum

Tsutomu Mita, Sang-Ho Hyon, and Taek-Kun Nam

**Abstract**—In order to control gymnastic and jumping robots, we will derive the complete analytical solution to the posture control problem of a two-link free flying object with initial angular momentum. We will show that the solution involves singular control and derive formulas to calculate the optimal switching condition, optimal terminal time and optimal trajectories. As an application, a high diving motion is simulated.

**Index Terms**—Acrobat robot, initial angular momentum, nonholonomic control, time optimal control.

### I. INTRODUCTION

The purpose of this paper is to derive the analytical time optimal posture control law for free flying planar objects having nonzero angular momentum. We plan to use it to build a parallel bar gymnastic robot and running robot in the next stage of our research. The solution also can be applied to the posture control problem of a two-link planar manipulator in the horizontal plane with a passive first link and an initial angular velocity.

There is much research treating the control of free flying objects with zero initial angular momentum, to name but a few, [1]–[6], where at least three degree of freedom (dof) is required to guarantee controllability. Especially, Mukherjee *et al.* [3] introduced the concept of geometric phase to control a three link space robot.

However, the problems treating in this paper are a little bit different from these since the motion of the free flying objects having nonzero angular momentum is described by an affine nonlinear system with the drift term having no equilibrium. Kamon *et al.* [7] formulated the posture control problem as a path planning problem and derived a minimum energy trajectory by numerical optimization method to simulate a three-dimensional (3-D) somersault motion. Godhavn *et al.* [8] converted the posture control problem to a bang-bang control problem and proposed a potential numerical computation algorithm to show a somersault motion of a planar diver. However, since these are numerical solutions, we cannot obtain the closed form control formulas which are needed for experiments. In addition, we cannot know the nature of the optimal solutions, e.g., we cannot tell when a particular solution becomes singular. Berkemeier *et al.* [9] dealt with a two-link hopping robot and solved the posture control problem by controlling the twist angle as a particular periodic time function.

The obtained time optimal solutions in this paper include simple closed form formulas of the control law. They also show that the problem leads to a singular optimal control problem depending upon the initial posture; the switching time is once when the singular solution does not occur while is twice when the singular solution is used. As an application, the somersault motion of a diver approximated by the two-link system is simulated.

Manuscript received June 19, 2000; revised November 27, 2000 and March 5, 2001. This paper was recommended for publication by Associate Editor H. Arai and Editor S. Hutchinson upon evaluation of the reviewers' comments.

The authors are with the Department of Control and Systems Engineering, Tokyo Institute of Technology, Meguro-ku, Tokyo, 152-0033 Japan (e-mail: mita@ctrl.titech.ac.jp; sangho@ctrl.titech.ac.jp; nam@ctrl.titech.ac.jp).

Publisher Item Identifier S 1042-296X(01)06736-2.

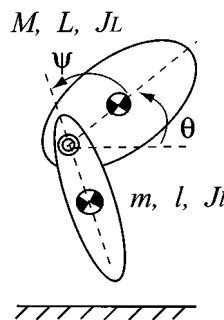


Fig. 1. Two-link free flying robot.

### II. STATEMENT OF PROBLEMS AND CANONICAL FORM

Consider the posture control problem of a planar free flying robot as shown in Fig. 1, where the robot is composed of the body and leg;  $\theta$  is the absolute angle of the body measured counterclockwise relative to the frame of inertia;  $\psi$  is the relative angle between the body and leg measured counterclockwise;  $L$  and  $l$  are the distances between the joint and the centers of mass (CM) of the body and the leg, respectively;  $M$  and  $J_L$  are the weight of the body and the moment of inertia of the body around its CM;  $m$  and  $J_l$  are those for the leg.

Suppose that the robot has a nonzero constant angular momentum  $P_0$  which is provided from the ground before takeoff as an initial angular momentum. Then the conservation law of angular momentum around CM of the whole robot becomes [9]

$$P_0 = (M_1 + A_1 \cos \psi)\dot{\theta} + (M_2 + A_2 \cos \psi)\dot{\psi} \quad (1)$$

where

$$\begin{aligned} M_1 &= J_L + J_l + \frac{mM(L^2 + l^2)}{m + M}, & A_1 &= 2A_2 \\ M_2 &= J_l + \frac{mMl^2}{m + M}, & A_2 &= \frac{mMlL}{m + M}. \end{aligned} \quad (2)$$

In the sequel, we assume that  $M_1 > A_1$  and  $A_2 \neq 0$ . Then, under the assumption  $P_0 \neq 0$ , (1) cannot be integrated and becomes a nonholonomic constraint. Note that when  $P_0 = 0$ , (1) turns to be an algebraic equation and  $\theta$  and  $\psi$  cannot be controlled independently. With a little modification of the parameters, (1) also describes a two-link manipulator in the horizontal plane with an unactuated first joint and initial angular velocity.

Defining  $\dot{\psi}$  as a control, (1) can be described by

$$\begin{bmatrix} \dot{\psi} \\ \dot{\theta} \end{bmatrix} = \begin{bmatrix} 0 \\ \frac{P_0}{M_1 + A_1 \cos \psi} \end{bmatrix} + \begin{bmatrix} 1 \\ -\frac{M_2 + A_2 \cos \psi}{M_1 + A_1 \cos \psi} \end{bmatrix} u \quad (3)$$

which is a nonlinear system with a drift term:

$$\dot{q} = f(q) + b(q)u; \quad q = (\psi, \theta)^T \quad (4)$$

having no equilibrium because  $f(q) \neq 0$  ( $\forall q$ ). Apparently, this system satisfies the locally accessible condition [6].

Since the rotational motion of the robot cannot be stopped when  $P_0 \neq 0$ , the control problem is to make  $q$  passing through a given reference state  $q_r = (\psi_r, \theta_r)^T$  at a given time  $T$ . Only  $\psi$  can be settled at  $\psi_r$  by putting  $u = 0$  after arrival to the reference state.

Since the translated motion of the robot cannot be controlled at all, we will not mention about it. Animals and gymnasts control their posture within the falling time.

If we can transform (3) to a system where the second entry of  $b(q)$  is zero, the corresponding state can be characterized as the state inde-

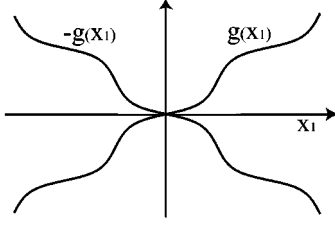


Fig. 2.  $g(x_1)$  and  $-g(x_1)$  when  $\psi_r = 0$ .

pendent of  $u$ . This can be possible only for the two-link robot and an immediate calculation derives the following canonical form:

$$\begin{bmatrix} \dot{x}_1 \\ \dot{x}_2 \end{bmatrix} = \begin{bmatrix} 0 \\ \frac{P_0}{M_1 + A_1 \cos(x_1 + \psi_r)} \end{bmatrix} + \begin{bmatrix} 1 \\ 0 \end{bmatrix} u \quad (5)$$

where  $x = (x_1, x_2)^T$  is the new coordinate defined by

$$x_1 = \psi - \psi_r, \quad x_2 = \theta + w(\psi) - (\theta_r + w(\psi_r)) \quad (6)$$

and [11]

$$\begin{aligned} w(\psi) &= \int_0^\psi \frac{M_2 + A_2 \cos p}{M_1 + A_1 \cos p} dp \\ &= \frac{A_2}{A_1} \psi + \frac{2(M_2 A_1 - M_1 A_2)}{A_1 \sqrt{M_1^2 - A_1^2}} \\ &\quad \times \tan^{-1} \left( \sqrt{\frac{M_1 - A_1}{M_1 + A_1}} \tan \frac{\psi}{2} \right). \end{aligned} \quad (7)$$

Then the control problem is transformed to drive  $x(0)$  to the origin 0 at the time  $T$ . Since (5) yields

$$\{M_1 + A_1 \cos(x_1 + \psi_r)\} \dot{x}_2 = P_0 \quad (8)$$

and  $M_1 + A_1 \cos(x_1 + \psi_r)$  is the moment of inertia around CM of the whole robot,  $x_2$  can be interpreted as the rotational angle around the CM of the whole robot.

Since the domain of  $\psi$  is defined as  $R^1 = (-\infty, \infty)$  for derivation of the control law and computer simulations, the continuity of the function  $\tan^{-1}(* \cdot \tan(\psi/2))$  in (7) at  $\psi = \pm n\pi$  becomes critical. To this end, as introduced in [4], we propose to replace  $\tan^{-1}(\cdot)$  in (7) by

$$k\pi + \tan^{-1} \left( \sqrt{\frac{M_1 - A_1}{M_1 + A_1}} \tan \frac{\psi - 2k\pi}{2} \right) \quad (9)$$

depending upon

$$(2k - 1)\pi \leq \psi < (2k + 1)\pi. \quad (10)$$

As the result,  $w(\psi)$  becomes a single-valued function just the same as  $g(x_1)$  depicted in Fig. 2.

Let's examine the nature of the canonical form (5) first by assuming  $P_0 > 0$ . Then, from  $M_1 > A_1$  and  $P_0 > 0$ , we can see that  $x_2(t)$  cannot move in the negative direction and the accessible region to the origin must satisfies

$$x_2(0) < 0. \quad (11)$$

Actually, this is shown to be sufficient below, when  $P_0 < 0$ , (11) is replaced by  $x_2(0) > 0$ .

### III. ANALYTICAL SOLUTION OF THE TIME OPTIMAL CONTROL PROBLEM

#### A. Optimal Control Problem and Solutions

We will solve the time optimal control problem for (5) and investigate the optimal trajectories. First of all, we define

$$p(x_1) := \frac{P_0}{M_1 + A_1 \cos(x_1 + \psi_r)} \quad (12)$$

in (5). The control problem is to minimize

$$J = \int_0^T dt = T \quad (13)$$

while bringing  $x(0)$  to  $x(T) = 0$  under the constraint  $|u| \leq u_m$ .

The Hamiltonian of this problem is

$$\begin{aligned} H &= 1 + \lambda^T \left[ \begin{bmatrix} 0 \\ p(x_1) \end{bmatrix} + \begin{bmatrix} 1 \\ 0 \end{bmatrix} u \right] \\ &= 1 + \lambda_1 u + \lambda_2 p(x_1) \end{aligned} \quad (14)$$

and the principle of optimality yields the following necessary conditions

$$u = -\text{sgn}(\lambda_1) u_m \quad (15)$$

$$\dot{\lambda} = -\frac{\partial H}{\partial x} = \begin{bmatrix} -\frac{\partial p(x_1)}{\partial x_1} \lambda_2 \\ 0 \end{bmatrix} \quad (16)$$

$$H(t) = 1 + \lambda_1 u + \lambda_2 p(x_1) = 0 \quad (\forall t). \quad (17)$$

Note that the bang-bang control law (15) holds only when the problem is regular, i.e.,  $\lambda_1$  is not identically zero for some time interval [10]. When it becomes singular, only (16) and (17) hold.

Since  $\dot{\lambda}_2 = 0$  in (16) yields  $\lambda_2 = \text{constant} := -\alpha$ , the regular problem reduces to find  $\lambda_1(0)$  and  $\alpha$  satisfying  $x(T) = 0$  under the conditions:

$$\dot{x}_1 = -\text{sgn}(\lambda_1) u_m \quad (18)$$

$$\dot{x}_2 = p(x_1) \quad (19)$$

$$\dot{\lambda}_1 = \alpha \frac{\partial p(x_1)}{\partial x_1} \quad (20)$$

$$H = 1 + \lambda_1 u - \alpha p(x_1) = 0 \quad (\forall t). \quad (21)$$

However, this problem can be solved analytically without seeking  $\lambda_1(0)$  and  $\alpha$  explicitly if we pay attention to the two integral manifolds made by  $u = \pm u_m$ .

Examine the case  $u = u_m$  ( $\lambda_1 < 0$ ) first. In this case, it follows from  $\dot{x}_1 = u_m$  that  $x_1$  increases monotonically. Besides, using  $\dot{x}_2/\dot{x}_1 = dx_2/dx_1 = p(x_1)/u_m$ ,  $x_2$  satisfies the following manifold

$$x_2 = \frac{g(x_1)}{u_m} + C_1, \quad (22)$$

where  $g_1(x_1)$  is described by

$$\begin{aligned} g(x_1) &= \int_0^{x_1} p(y) dy \\ &= \frac{2P_0}{\sqrt{M_1^2 - A_1^2}} \tan^{-1} \left( \sqrt{\frac{M_1 - A_1}{M_1 + A_1}} \tan \frac{x_1 + \psi_r}{2} \right) \end{aligned} \quad (23)$$

provided all constants are collected to make one integral constant  $C_1$ . When calculating  $\tan^{-1}(\cdot)$ , we will use (9) and (10).

Similarly, when  $u = -u_m$  ( $\lambda_1 > 0$ ), we have another manifold

$$x_2 = \frac{-g(x_1)}{u_m} + C_2. \quad (24)$$

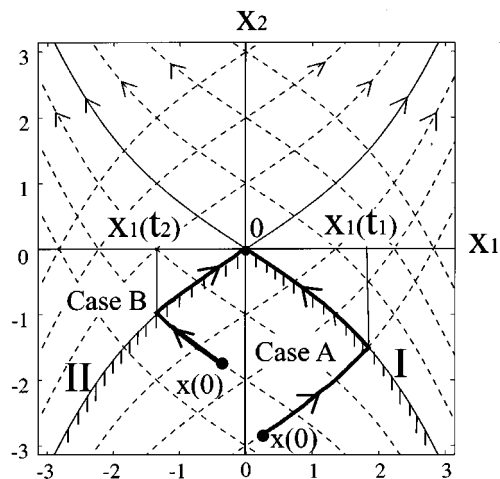


Fig. 3. Switching line I, II, and optimal trajectories.

The integral constants  $C_1$  and  $C_2$  must be adjusted for (22) and (24) to pass through designated states.

We will treat the case  $\psi_r = 0$  to save the length of the paper, then  $g(x_1)$  is given by a single-valued function passing through the origin as depicted in Fig. 2. Furthermore, as shown in Fig. 3, (22) and (24) draw a bunch of curves rising in the right-hand side (RHS) and left-hand side (LHS) directions, respectively, when the integral constants  $C_1$  and  $C_2$  vary. We'll refer to the two manifolds, denoted by I and II in Fig. 3, passing through the origin as the *switching line* hereafter. From Fig. 3, we can see that we can find a controlled trajectory only when  $x_2(0)$  exists in the region under the switching line I and II (the region is marked by slashes). The control strategy is as follows. As is in Case A, when  $x_1(0) > 0$ , we first choose  $u = u_m$  to ride the state on the manifold rising in the RHS direction, then switch the control to  $u = -u_m$  when the state reaches the switching line I. Similarly, as is in Case B, when  $x_1(0) < 0$ , we first choose  $u = -u_m$ , followed by  $u = u_m$  when the state reaches the switching line II. When  $x_1 = 0$ , we can choose either controls in Case A or Case B,  $x_1 = 0$  gives the boundary between Case A and Case B.

Note that we have infinitely number of choices of the control sequences if we don't care about the optimality. However, the final choice must be riding the state on the switching line I or II in the fourth quadrant or third quadrant, respectively.

In Section IV, we will prove the following theorem.

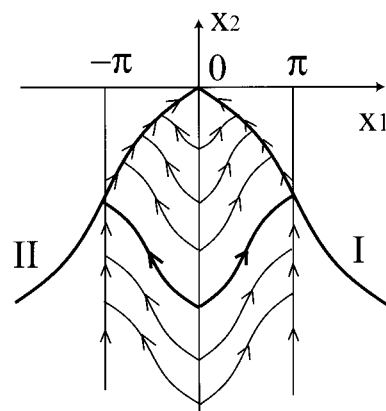
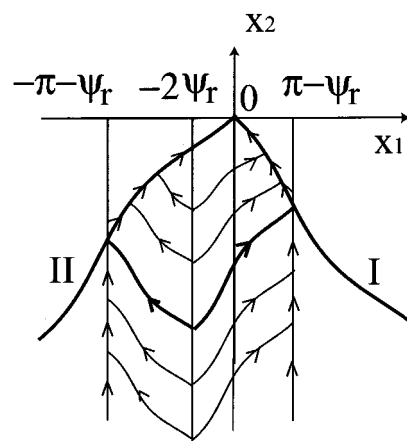
*Theorem 1:*

- 1) when  $-\pi < x_1(t) < \pi$ , the mentioned control strategy is optimal;
- 2) when  $x_1(t) = -\pi$  or  $x_1(t) = \pi$  happens, which corresponds to  $\psi = \pm\pi$ , the control problem becomes singular, and, as is shown in Fig. 4, the optimal control is given by  $u = 0$  before riding the state on the switching lines I or II;
- 3) when  $\psi_r \neq 0$ , the boundary of Case A and Case B is given by  $x_1 = -2\psi_r$  as shown in Fig. 5.

From this theorem, we can see that the control strategy explained in Fig. 3 is optimal only when  $x(0)$  is located inside the area enclosed by the bold face curves depicted in Figs. 4 and 5. We call this area a *basic region*.

Note also that the robot rotates by the fastest angular velocity with holding the leg upon the body to minimize the moment of inertia of the robot in the singular period because  $\psi$  becomes  $\pm\pi$ .

Before concluding this section, let's examine the role of  $u_m$  and accessible region. When  $u_m$  is chosen bigger, it follows from (22) and (24) that the lines I and II becomes flat and close to  $x_1$  line. Therefore, the region of  $x_2(0)$  which can be brought to the origin approaches


 Fig. 4. Optimal trajectories when  $\psi_r = 0$ .

 Fig. 5. Optimal trajectories when  $\psi_r \neq 0$ .

$x_2 < 0$ . Since (11) has been shown to be necessary before, (11) is the necessary and sufficient condition of the initial state which can access the origin by the control.

However, in the physical world,  $x_2$  is counted by mod  $2\pi$ . Therefore, even when  $x_2(0) > 0$ , predetermining an integer  $k$  satisfying  $\bar{x}_2 = x_2 - 2k\pi < 0$  and treating  $(x_1(0), \bar{x}_2(0))$  as a new initial state will get around the limitation (11) at the expense of more time to reach the origin. We have to introduce a similar shift to  $x_1$  to express it in the interval  $-\pi \sim \pi$ .

### B. Optimal Switching Conditions

We will derive the switching condition as well as the optimal switching time when  $x(0)$  lies in the basic region by making use of Fig. 3. This will be used for practical implementation of the control law.

When  $u = \pm u_m$ ,  $\dot{x}_1 = \pm u_m$  yields the solution

$$x_1(t) = \pm u_m t + x_1(0) \quad (25)$$

which shows that (the change of  $x_1/u_m$ ) gives the transition time when  $u = \pm u_m$ . This fact will be used frequently without mentioning.

Now let us define the switching time and the terminal time of the trajectory in Case A by  $t_1$  and  $T_A$ , then

$$\begin{aligned} x_1(t_1) &= u_m t_1 + x_1(0) \\ x_1(T_A) &= -u_m(T_A - t_1) + x_1(t_1) \end{aligned} \quad (26)$$

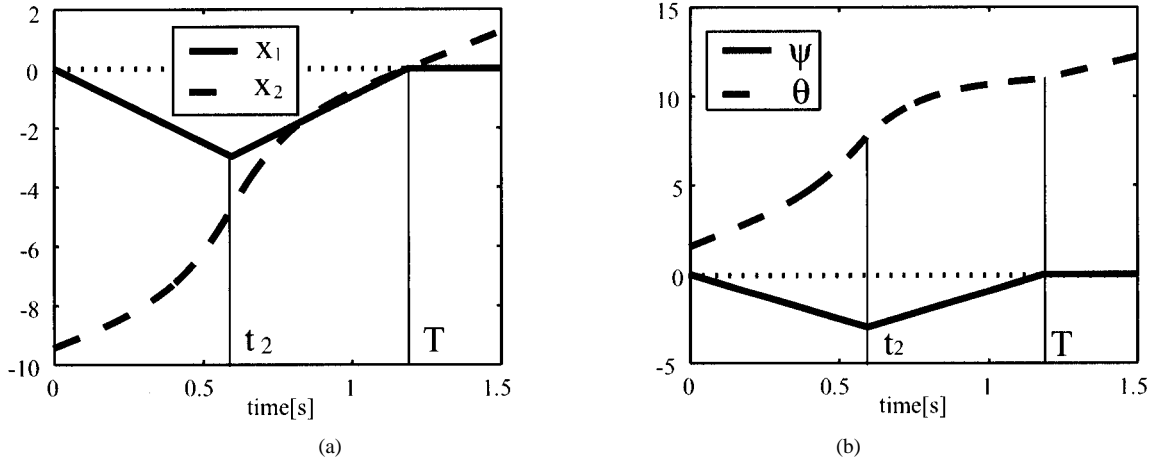


Fig. 6. Simulation results (a)  $x$  coordinate (b)  $q$  coordinate.

hold and from the condition  $x_1(T_A) = 0$ , we have

$$T_A = 2t_1 + \frac{x_1(0)}{u_m} = \frac{2x_1(t_1) - x_1(0)}{u_m}. \quad (27)$$

On the other hand, since  $x(0)$  lies on the manifold (22) and the switching line I passes through the origin, we have

$$C_1 = x_2(0) - \frac{g(x_1(0))}{u_m}, \quad C_2 = \frac{g(0)}{u_m}, \quad (28)$$

respectively. Furthermore, since  $x(t_1)$  lies on the both of the manifolds

$$\begin{aligned} x_2(t_1) &= \frac{g(x_1(t_1))}{u_m} + x_2(0) - \frac{g(x_1(0))}{u_m} \\ x_2(t_1) &= -\frac{g(x_1(t_1))}{u_m} + \frac{g(0)}{u_m} \end{aligned} \quad (29)$$

hold. Therefore, solving (29) to obtain

$$g(x_1(t_1)) = -\frac{u_m}{2}x_2(0) + \frac{g(x_1(0))}{2} + \frac{g(0)}{2} \quad (30)$$

$$x_2(t_1) = \frac{x_2(0)}{2} - \frac{g(x_1(0))}{2u_m} + \frac{g(0)}{2u_m}. \quad (31)$$

Using the fact that  $g(x_1)$  is a single-valued function, solving (30) gives  $x_1(t_1)$  and (27) provides  $T_A$ .

Moreover, the first equation in (26) gives the following switching time

$$t_1 = \frac{x_1(t_1) - x_1(0)}{u_m}. \quad (32)$$

Similarly, in the Case B, if the switching time and terminal time are defined by  $t_2$  and  $T_B$ , from

$$\begin{aligned} x_1(t_2) &= -u_m t_2 + x_1(0) \\ x_1(T_B) &= u_m(T_B - t_2) + x_1(t_2) = 0 \end{aligned} \quad (33)$$

we will obtain

$$T_B = \frac{-2x_1(t_2) + x_1(0)}{u_m} \quad (34)$$

and

$$g(x_1(t_2)) = \frac{u_m}{2}x_2(0) + \frac{g(x_1(0))}{2} + \frac{g(0)}{2} \quad (35)$$

$$x_2(t_2) = \frac{x_2(0)}{2} + \frac{g(x_1(0))}{2u_m} - \frac{g(0)}{2u_m}. \quad (36)$$

Therefore, we can calculate  $x_1(t_2)$  from (35). Then, (34) leads to  $T_B$ . The  $t_2$  can be derived from the first equation of (33) as

$$t_2 = \frac{-x_1(t_2) + x_1(0)}{u_m}. \quad (37)$$

In the practical implementation of the control law, making use of  $x_2(t_1)$  and  $x_2(t_2)$  as the switching conditions may be more robust than using  $t_1$  and  $t_2$ .

As for the singular control period, it follows from  $x_1 = \pm\pi$ ,  $u = 0$  and (19) that we have

$$\dot{x}_2 = \frac{P_0}{M_1 - A_1} := K. \quad (38)$$

Therefore, the transition time in the singular period is given by the division of the change of  $x_2$  by  $K$ . Furthermore, even Fig. 3 corresponds to the case  $\psi_r = 0$ , the above derivation is independent of  $\psi_r$  and we can apply all the results, from (25)–(38), to the case  $\psi_r \neq 0$ .

*Example:* We will simulate the motion of a planar diver approximated by two links with the parameters

$$\begin{aligned} M &= 30 \text{ (kg)}, & L &= 0.75 \text{ (m)}, & J_L &= 5.0 \text{ (kg} \cdot \text{m}^2) \\ m &= 25 \text{ (kg)}, & l &= 0.8 \text{ (m)}, & J_t &= 4.5 \text{ (kg} \cdot \text{m}^2) \\ P_0 &= 170 \left( \frac{\text{kg} \cdot \text{m}^2}{\text{s}} \right), & u_m &= 5 \left( \frac{1}{\text{s}} \right) \end{aligned}$$

when  $q_0 = (0, \pi/2)^T$  and  $q_r = (0, 7\pi/2)^T$ , which correspond to  $x(0) = (0, -3\pi)$ , the optimal control law provides the switching conditions  $x_1(t_2) = -2.9694$ ,  $x_2(t_2) = -4.7124$  and  $t_2 = 0.5939$  (s) (corresponding to Case B) and the terminal time  $T = 1.1878$  (s). In this case, the robot performs one and half somersault. The time responses in terms of  $x$  and  $q$  are depicted in Fig. 6(a) and (b), respectively, while Fig. 7 shows the animation. The translated motions have been simulated under the conditions  $V_X = 1.5$  (m/s) and  $V_Y = 1.8$  (m/s), where  $V_X$  and  $V_Y$  are initial speeds of the CM of the whole robots.

In this problem setting, the minimum time control tells how long does it take at least to complete a specified motion within a given input magnitude  $u_m$ .

*Remark 1:* In the case where a real robot cannot bend the leg  $\pm\pi/2$ , the following method may be applied if we do not care about the optimality much. Draw the singular line on  $\psi = \pi - a$  ( $a > 0$ ) instead of  $\psi = \pi$ . When  $x_1$  comes across this new line, keep  $u = 0$  until the state rides on the switching line I followed by  $u = -u_m$ . The maximum velocity  $u_m$  of the joint depends on the requested acrobatic performance,  $P_0$  and the falling time. Some compromise will be required in the experiment.

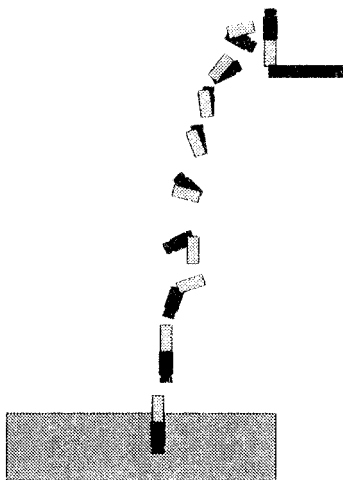


Fig. 7. The animation.

#### IV. PROOF OF THEOREM 1

##### A. Proof of the Item 1 and Item 2

We will prove the item 1 and item 2 in Theorem 1.

To this end, we will analyze the response of  $\lambda_1$  and (21).

Let's consider the case where  $\lambda_1$  is not identically zero, first.

If  $\lambda_1 < 0$ , (18) leads to  $u = u_m$  and it follows from  $\dot{x}_1 = u_m \rightarrow dt = dx_1/u_m$  that  $x_1$  increases with the time and we can integrate (20) as

$$\begin{aligned} \lambda_1 &= \alpha \int^t \frac{dp(x_1)}{dx_1} dt = \frac{\alpha}{u_m} \int^{x_1(t)} dp(x_1) \\ &= \frac{\alpha}{u_m} p(x_1(t)) + K_1. \end{aligned} \quad (39)$$

Substituting this into (21) yields

$$1 + u_m \left[ \frac{\alpha}{u_m} p(x_1) + K_1 \right] - \alpha p(x_1) = 0 \quad (40)$$

from which  $K_1 = -1/u_m$  is obtained. Therefore,  $\lambda_1(t)$  is expressed by

$$\lambda_1(t) = - \left( \frac{1 - \alpha p(x_1(t))}{u_m} \right) \quad (41)$$

as a function of  $x_1(t)$ .

Similarly, when  $\lambda_1 > 0$ ,  $u = -u_m$  leads to that  $x_1$  decreases with the time and we can conclude

$$\lambda_1(t) = \left( \frac{1 - \alpha p(x_1(t))}{u_m} \right). \quad (42)$$

It follows from the continuity of  $\lambda_1(t)$  that (41) must intersect (42). Since the two  $\lambda_1$ 's are the same except for their signs, they intersect only on the  $x_1$  axis as shown in Fig. 8(a). Therefore, the input is switched at these intersection points. Let us denote one of the intersection point by  $x_1 = x_{1s}$  ( $x_{1s}$  corresponds to  $x_1(t_1)$  or  $x_1(t_2)$  in the previous chapter). Equating two  $\lambda_1$ 's at these points, we have

$$p(x_{1s}) = \frac{1}{\alpha} \quad (43)$$

where  $\alpha$  may be determined by the initial condition. It will be seen from Fig. 8(a) that  $x_{1s}$  must satisfy  $|x_{1s}| \leq \pi$  and only one switching instant is allowed before  $x_1$  arrive at 0 from  $x_1(0)$ . The reason is as follows.

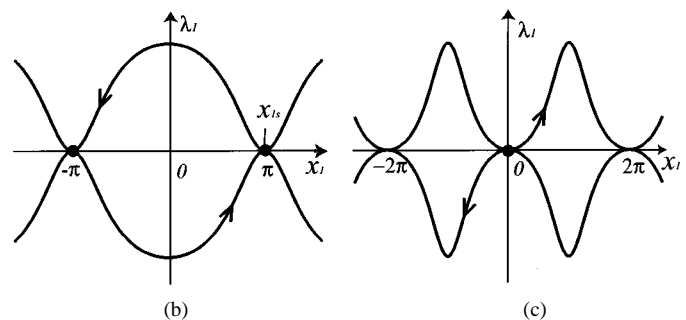
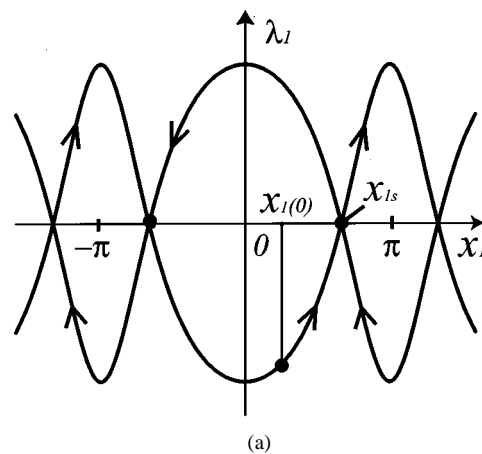


Fig. 8. Function  $\lambda_1$  versus  $x_1$  (a)  $x_{1s} \neq \pm\pi$  (ordinary solution). (b)  $x_{1s} = \pm\pi$  (singular solution). (c)  $x_{1s} = 0$  (trivial solution).

If  $x_1$  would move across  $x_{1s}$ , it should move to the next intersection point which increases the travelling time to  $x_1 = 0$ . Therefore

$$|x_1(t)| \leq |x_{1s}| \leq \pi \quad (44)$$

must hold.

Next, suppose that  $\lambda_1$  becomes identically zero for some finite time interval. In this case, since  $H$  is independent of  $\lambda_1$ ,  $u$  cannot be determined from (15) and the problem becomes singular [10]. However, from Fig. 8(a), if there exists such a  $\lambda_1$ , it should be at the intersection point such that  $\lambda_1(t) = 0$  and  $x_1(t) = x_{1s}$  hold for some period.

Besides, in the singular period, the derivatives of  $\lambda_1(t)$  of any order must be zero. Its first and second derivatives are given by

$$\dot{\lambda}_1 = \alpha \frac{dp(x_1)}{dx_1}, \quad \ddot{\lambda}_1 = \alpha \frac{d^2p(x_1)}{dx_1^2} \dot{x}_1 \quad (45)$$

where

$$\frac{dp(x_1)}{dx_1} = \frac{P_0 A_1 \sin x_1}{(M_1 + A_1 \cos x_1)^2}. \quad (46)$$

Therefore, the following conditions

$$\begin{aligned} x_1 = x_{1s} = \pm\pi, \text{ and } \dot{x}_1 = u = 0 \\ x_1 = x_{1s} = 0, \text{ and } \dot{x}_1 = u = 0 \end{aligned} \quad (47)$$

make them zero and the converse also holds. It is direct to check that  $\lambda_1^{(i)}(t) (\forall i \geq 3) = 0$  hold under (47). In addition, when  $\lambda_1(t) = 0$ , Hamiltonian (21) becomes

$$H = 1 - \alpha p(x_1) \quad (48)$$

which is ensured to be zero under the conditions (43) and (47). Therefore (43) and (47) are the necessary conditions for singular control.

Let us consider the case  $x_1 = x_{1s} = \pm\pi$  and  $u = 0$ . This corresponds to the  $\lambda_1$  depicted in Fig. 8(b), where the robot rotates by the fastest speed as stated before.

Then consider the case  $x_1 = x_{1s} = 0$  and  $u = 0$  which corresponds to the  $\lambda_1$  shown in Fig. 8(c). It will be a singular solution only if  $x_2(0) = 0$  because, when  $x_2(0) < 0$ ,  $u = 0$  leads to a trajectory keeping  $x_1 = 0$  before the convergence which contradicts the optimal trajectory in the basic region shown in Fig. 3. However, the solution  $x_1 = x_2 = 0$  and  $u = 0$  is trivial and we cannot count this as a singular solution since itself is on the reference state.

Therefore, the following conclusions are obtained. When  $x(0) \neq 0$  and  $|x_1| < \pi$ , the singular solution does not occur and one time switching is optimal; when the state comes across  $|x_1| = \pi$ ,  $u = 0$  gives the singular control and the optimal trajectory is produced by two time switchings as shown in Fig. 4, since the continuity of the trajectory must hold. ■

### B. Proof of the Item 3

We will prove that  $x_1(0) = -2\psi_r$  renders  $T_A = T_B$  when  $\psi_r \neq 0$ . Since Fig. 3 can be applied even to the case  $\psi_r \neq 0$  as mentioned at the end of Section III, it follows (27) and (34) that  $T_A = T_B$  holds only if

$$x_1(t_1) + x_1(t_2) = x_1(0) \quad (49)$$

where  $x_1(t_1)$  and  $x_1(t_2)$  will be provided by solving (30)–(35). Thus, the problem is to show that (49) holds when  $x(0) = -2\psi_r$ .

An addition of (30) to (35) gives

$$g(x_1(t_2)) + g(x_1(t_1)) = g(x_1(0)) + g(0). \quad (50)$$

To make description simpler, we denote  $g(x) = g_0(x + \psi_r)$ , then  $g_0(x)$  becomes an oddly symmetrical function passing through the origin as we may imagine in Fig. 2.

When  $x_1(0) = -2\psi_r$ , it follows from

$$\begin{aligned} g(x_1(0)) &= g(-2\psi_r) = g_0(-\psi_r) = -g_0(\psi_r) \\ g(0) &= g_0(\psi_r) \end{aligned} \quad (51)$$

that the RHS of the first equation in (50) is zero, and (50) can be rewritten as

$$g_0[x_1(t_1) + \psi_r] = -g_0[x_1(t_2) + \psi_r] \quad (52)$$

using  $g_0$ . However, since  $g_0(x_1)$  is an oddly symmetrical single-valued function, (52) is satisfied only if

$$x_1(t_1) + \psi_r = -(x_1(t_2) + \psi_r). \quad (53)$$

This becomes (49) when  $x_1(0) = -2\psi_r$ .

In [12], we have even proven that  $T_A < T_B$  holds when  $-2\psi_r < x_1(0) < \pi - \psi_r$ . ■

## V. CONCLUSION

We have derived an analytical solution to the minimum time optimal control problem of a two-link flying robot having nonzero angular momentum. For the posture control of general  $n$  link robots, we can apply obtained results after fixing  $n - 2$  joint angles. The optimality is not guaranteed in this methodology. We are now constructing a parallel bar gymnastic robot which can perform a somersault.

## REFERENCES

- [1] Y. Nakamura and R. Mukherjee, "Nonholonomic path planning of space robots via a bidirectional approach," *IEEE Trans. Robot. Automat.*, vol. 7, pp. 500–514, 1991.
- [2] H. Krishnan, M. Reyhanoglu, and H. McClamroch, "Attitude stabilization of a rigid spacecraft using two control torques: a nonlinear control approach based on the spacecraft attitude dynamics," *Automatica*, vol. 30, no. 6, pp. 1023–1027, 1994.
- [3] R. Mukherjee and M. Kamen, "Almost smooth time-invariant control of a planar space multibody systems," *IEEE Trans. Robot. Automat.*, vol. 15, pp. 268–280, 1999.
- [4] T. Ikeda, T. K. Nam, T. Mita, and B. D. O. Anderson, "Variable constraint control of underactuated free flying robots," in *Proc. IEEE Conf. Decision Contr.*, 1999, pp. 2539–2544.
- [5] I. Kolmanovsky and N. H. McClamroch, "Developments in nonholonomic control problems," *IEEE Contr. Syst. Mag.*, vol. 15, pp. 20–36, 1995.
- [6] R. M. Murray, Z. Li, and S. Sastry, *A Mathematical Introduction to Robotic Manipulation*. Boca Raton, FL: CRC, 1994.
- [7] M. Kamen and K. Yoshida, "3D attitude control methods for free-flying dynamic system with initial angular momentum," *J. Robot. Soc. Japan*, vol. 16, no. 2, pp. 223–231, 1998.
- [8] J. M. Godhavn, A. Balluchi, L. S. Crawford, and S. Sastry, "Steering of a class of nonholonomic systems with drift terms," *Automatica*, vol. 35, pp. 837–847, 1999.
- [9] M. D. Berkemeier and R. S. Fearing, "Control of a two-link robot to achieve sliding and hopping gaits," in *Proc. IEEE Conf. Robot. Automat.*, 1992, pp. 286–291.
- [10] M. Athans and P. L. Falb, *Optimal Control*. New York: McGraw-Hill, 1966, pp. 481–493.
- [11] S. Moriguchi, K. Udagawa, and S. Ichimatsu, *Mathematical Formula II*. Tokyo: Iwanami, 1987.
- [12] T. Mita, S. H. Hyon, and T. K. Nam, "Analytical time optimal control solution for free flying objects with drift term," in *Proc. 3rd ITTech. COE/SMS Symp.*, 2000, pp. 72–82.